Journal of Nuclear Materials 386–388 (2009) 712–715

Contents lists available at ScienceDirect

Journal of Nuclear Materials

journal homepage: www.elsevier.com/locate/jnucmat

Initial characterization of V–4Cr–4Ti and MHD coatings exposed to flowing Li

B.A. Pint *, S.J. Pawel, M. Howell, J.L. Moser, G.W. Garner, M.L. Santella, P.F. Tortorelli, F.W. Wiffen, J.R. DiStefano

Materials Science and Technology Division, Oak Ridge National Laboratory, P.O. Box 2008, Oak Ridge, TN 37831-6156, USA

A B S T R A C T

A mono-metallic V–4Cr–4Ti thermal convection loop was operated in vacuum (~10^{-5} Pa) at a maximum Li temperature of 700 °C for 2355 h and Li flow rate of 2–3 cm/s. Two-layer, physical vapor deposited Y_2O_3–vanadium, electrically insulating coatings on V–4Cr–4Ti substrates as well as tensile and sheet specimens were located in the flow path in the hot and cold legs. After exposure, specimens at the top of the hot leg showed a maximum mass loss equivalent to ~1.3 μm of metal loss. Elsewhere, small mass gains were observed on the majority of specimens resulting in an increase in hardness and room temperature yield stress and a decrease in ductility consistent with the observed uptake of N and C from the Li. Specimens that lost mass showed a decrease in yield stress and hardness. Profilometry showed no significant thickness loss from the coatings.

1. Introduction

One of the critical unresolved issues for the vanadium–lithium blanket concept [1,2] (and any liquid metal concept) in a deuterium/tritium fueled fusion reactor [3,4] is the need to reduce the pressure drop associated with the magnetohydrodynamic (MHD) effect of a conducting liquid flowing across the magnetic field lines. One solution to the MHD problem is to decouple the structure wall from the liquid metal with an electrically insulating coating or flow channel insert (FCI) [5]. This coating application requires a thin, crack-free [6], durable layer with a relatively high electrical resistance [7]. While a 'self-healing' layer is possible in corrosion where a re-passivation can occur with the re-formation of a surface oxide, this concept is not applicable to functional (i.e. electrically resistant) coatings because a defect that shorts the coating and fills with liquid metal is unlikely to 'heal'. Therefore, a robust coating system or a FCI is needed for this application. Due to incompatibility between Li and virtually all candidate insulating oxides [8–12], the current focus of the US MHD coating program [10–12] is on evaluating the compatibility of durable, multi-layer coatings [7,13] where a vanadium overlayer prevents direct contact between the insulating oxide layer and Li. This concept shifts the compatibility concern from the oxide layer to the thin vanadium overlayer. In order to verify that a thin, ~10 μm, V layer is sufficiently compatible with Li to function in a long-term situation, a mono-metallic thermal convection loop was designed and built to expose thin V overlayers to flowing Li. The loop was operated with a peak temperature of ~700 °C for 2355 h. Initial characterization of the coatings and V–4Cr–4Ti specimens in the loop are presented. Additional characterization of the coatings will be presented in future publications.

2. Experimental procedure

A harp-shaped thermal convection loop was constructed of drawn tubing made from the large US heat of V–3.8 wt%Cr–3.9%Ti (Heat# 832665 made at Wah Chang, Albany, OR) [14] with an outer diameter of 19 mm and a 1.6 mm wall thickness. The hot and cold legs were ~85 cm long and the top and bottom legs were ~33 cm long with a fill/expansion tank at the top of the hot leg. The loop was fabricated using gas tungsten arc welding in an Ar-filled glove box and state-of-the-art expertise [15]. The loop contained four thermal wells that extended ~5 mm into the flow path and contained type K thermocouples. The experiment was conducted in a stainless steel vacuum chamber. The loop was heated by three Mo wire furnaces, two on the hot leg and one on the Li tank. A total of 18 type K and 2 type S thermocouples were used to control the furnaces and monitor the temperatures around the loop. Wire and specimens all made from the same V–4Cr–4Ti heat formed ~80 cm long chains that were placed in the hot and cold legs. The 29 specimens in each chain consisted of alternating interlocked tabs (31 × 13 × 0.9 mm), which held the chain in the center of the tube, and pairs of miniature tensile specimens (type SS-3: 25 × 4 × 0.9 mm). Prior to exposure, the tensile specimens were vacuum annealed for 1 h at 1050 °C. The tab specimens were not annealed and had a fine-grained, cold-rolled microstructure. Specimen mass was measured on a microbalance with a ±0.01 mg/cm^2 error. Six of the exposed tabs had an electron-beam physical vapor deposited (EB-PVD) Y_2O_3 coating completely covered by an outer

* Corresponding author. Tel.: +1 865 576 2897; fax: +1 865 241 0215.
E-mail address: pintba@ornl.gov (B.A. Pint).

0022-3115/$ - see front matter © 2008 Elsevier B.V. All rights reserved.
doi:10.1016/j.jnucmat.2008.12.295

layer of unalloyed vanadium [11,12]. The coatings were made in two batches [16] and the unexposed coating thicknesses are shown in Table 1.

Sticks of Li (as-received batch: <100 ppmw N, 95 ppmw C and 950 ppmw O) [12] totaling ~275 g were loaded into the tank in a glove box and the lid of the tank was welded shut. The loop and tank were then evacuated with a roughing pump, leak checked and valved off. The loop was placed in the vacuum chamber and instrumented using Ta foil to hold the thermocouples and prevent them from direct contact with the V–4Cr–4Ti tubing. After baking for 48 h at 150 °C, the chamber achieved a base vacuum of 4×10^{-6} Pa (5×10^{-8} Torr) as measured on a vacuum gauge located on the chamber wall opposite the vacuum pump. The loop was then slowly preheated to ~250 °C while maintaining the chamber pressure at ~2×10^{-4} Pa using the hot leg heaters and resistively heating a W wire insulated with ceramic beads on the cold leg. After further heating the hot leg, a drastic increase in cold leg temperatures suggested the start of Li flow. After stabilization, temperature was subsequently controlled by maintaining the thermal well at the top of the hot leg at 700 ± 10 °C. Operation continued for a total of 2355 h and stopped due to a weather-related power outage. Temperatures in the four thermal wells are shown in Fig. 1. The chamber pressure initially spiked above 5×10^{-4} Pa but then continued to drop during exposure, reaching the desired <10^{-5} Pa by 400 h, Fig. 1. A much larger than expected temperature gradient was observed during the first 1248 h phase of operation. Initially, the difference between the top and bottom of the hot leg was 340 °C and slowly increased to almost 400 °C, Fig. 1. Using thermocouples to measure the movement of a hot spot created by a pair of SiC heating elements, the Li velocity was estimated to be ~2 cm/s during the first phase. After an unexplained upset that occurred between 1248 and 1262 h, Fig. 1, the cold leg temperatures increased and the gradient was only ~225 °C suggesting a faster Li velocity of >3 cm/s (based on the lower T gradient) which was similar to the velocity measured in the stainless steel test loop operated at ~550 °C [17]. However, the higher cold leg temperatures during the second operation phase prevented an accurate velocity measurement. The inability to maintain the peak temperature at 700 °C for the second operational phase (Fig. 1) was subsequently attributed to a loose furnace connection. One hypothesis for the high first phase ΔT is that the Li flow was restricted by the specimen chain and that specimen movement or the chain breaking (which was *not* observed during disassembly) allowed more rapid Li flow during the second phase. Additional operational details are provided elsewhere [18].

After the experiment ended, the chamber was opened and the loop inverted and re-instrumented. The chamber was then pumped down and the loop was heated to ~400 °C allowing the Li to drain back into the tank. The loop was then cut open in an Ar-filled glove box. The top tab specimens were not located below the cross-over joints in the hot and cold leg as designed and therefore could have restricted Li flow. The specimen chains were partially removed from the tubing and residual Li was removed using liquid ammonia followed by soaking in ethanol and then water.

Initial characterization of the specimens and tubing included metallographic cross-sections, hardness (Vickers, 300 g) measurements, chemical analysis using combustion and inductively coupled plasma analysis, and room temperature tensile testing at 10^{-3} s^{-1} strain rate. Selected specimens were examined using scanning electron microscopy (SEM) equipped with energy dispersive X-ray (EDX) analysis. The EB-PVD coatings were examined by SEM/EDX, contact profilometry and X-ray diffraction (XRD).

Table 1
Profilometry data of the V/Y_2O_3 coatings on V–4Cr–4Ti substrates after exposure to flowing Li for 2355 h in a V–4Cr–4Ti loop with a maximum temperature of 700 °C.

Location	Batch 1		Batch 2	
	V layer	Y_2O_3 layer	V layer	Y_2O_3 layer
Unexposed (μm)	9	13	10	17
Top hot leg	8	12		
Top cold leg	8	11		
Middle cold leg	7	12		
Bottom cold leg			10	15
Bottom hot leg			9	17
Middle hot leg			9	16
As-deposited*	7.4 ± 0.3	11.7 ± 0.5	9.9 ± 0.4	15.7 ± 0.9

* Ref. [16].

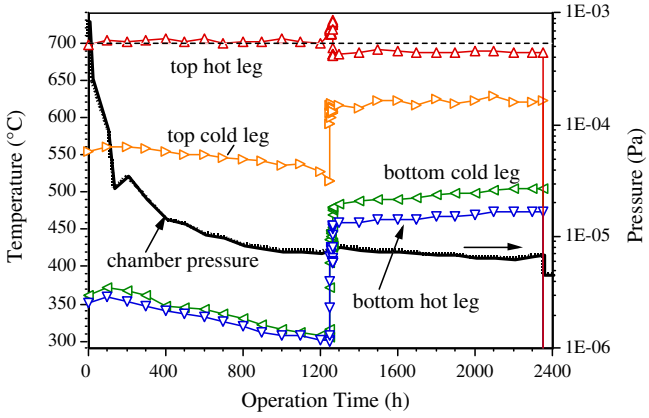

Fig. 1. Temperatures and vacuum pressure during the loop operation. Two phases of operation occurred due to an unexplained upset between 1248 and 1262 h.

3. Results and discussion

Fig. 2 shows the mass change data for both specimen chains with the nominal temperature profiles in the hot and cold legs assuming a linear temperature profile between the thermal wells. Mass losses in seven specimens from the hot leg were consistent with dissolution of metal (maximum ~0.6 mg/cm^2 is equivalent

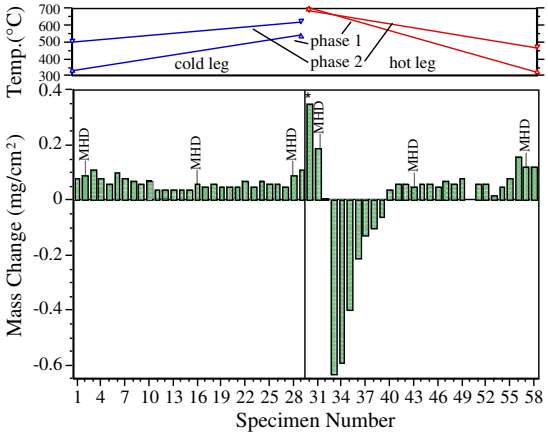

Fig. 2. Specimen mass gain for V–4Cr–4Ti specimens in the hot and cold leg of the mono-metallic loop along with the temperature that the specimens saw during the two phases of operation assuming a linear profile. In the hottest section of the loop, mass losses were observed, elsewhere, small mass gains were measured. The specimen at the top of the hot leg, marked by ∗, may have been above the Li flow path.

to 1 μm vanadium) and/or loss of interstitials such as oxygen. Assuming linear kinetics, the maximum observed loss is equivalent to ~2.5 mg/m^2 h which is similar to the rate reported previously at 538 °C for V–15Cr–5Ti with Li + 50 ppm N in a pumped loop (1 l/min) [19]. However, the results in that study were complicated by the use of a stainless steel loop. Prior results in a mono-metallic loop at 700 °C reported small mass gains after 1000 h [20].

Three specimens at the top of the hot leg did not show a mass loss, Fig. 2, which may be explained by temperature or Li flow differences. As mentioned previously, the chain was not positioned in the loop as designed and the first specimen in the chain (* in Fig. 2) appeared to be above the Li flow path, which may explain its high mass gain (i.e. higher interstitial pickup and/or less metal transfer). The second and third specimens appeared to be within the Li flow path although they were located above the hot leg furnace about ~2 cm from the hot leg thermal well where the 700 °C temperature was measured. Elsewhere in both legs, all of the specimens showed a small mass gain. The location of the six EB-PVD coated specimens are shown in Fig. 2, and each had a mass gain comparable to neighboring specimens.

Chemical analyses of the interstitial contents for selected tab specimens at the top, bottom and middle of the hot and cold leg are shown in Table 2. As expected, there was a decrease in the O content for all of the specimens and an increase in the N and C content. However, that effect was particularly strong in the hottest section where the O content decreased to 20 ppmw and the N content increased to 1590 ppmw. There was no significant change in the V, Cr or Ti contents measured. Table 2 also shows the measured and calculated mass change based on the chemistry change. The small mass change observed in most of the specimens is likely associated with the uptake of N and C minus the decrease in O. However, the mass gains in the coldest parts of the loop are not explained by this uptake and may be due to a small amount of metal deposition, e.g. a 0.06 mg/cm^2 mass gain would be equivalent to a ~100 nm layer of metal. For the highest temperature specimen analyzed from the hot leg, the large increase in N content resulted in a calculated net mass gain, suggesting that the metal loss may have been on the order of 0.8 mg/cm^2 or ~1.3 μm.

Fig. 3 shows results from room temperature tensile tests of specimens from the hot and cold legs as well as average values for unexposed specimens from the same specimen batch which have similar properties to prior studies [21–23]. The 0.2% yield and ultimate tensile strengths increased in specimens as the exposure temperature decreased, Fig. 3(a). The mass gain and associated N and C increase for many of these specimens suggest interstitial hardening as a mechanism to increase the yield and ultimate tensile stresses. The variation with temperature is likely due to thermal ageing during the 2355 h exposure. The specimens from the hot leg with mass losses showed a large decrease in yield strength, which is not consistent with the large N increase but is consistent with the large drop in O content, Table 2. In Fig. 3(b), modest decreases in the uniform and total elongations also were observed compared to unexposed specimens. These ductility values are somewhat higher than were previously reported [20]. Additional tensile specimens will be tested at 500 °C to compare to prior work on Li-exposed material [24].

Fig. 4 shows the change in average hardness (from a starting value of 204 ± 6 Hv for the starting unannealed cold-rolled material) and mass for tab specimens as a function of nominal average temperature based on their location in the specimen chain and

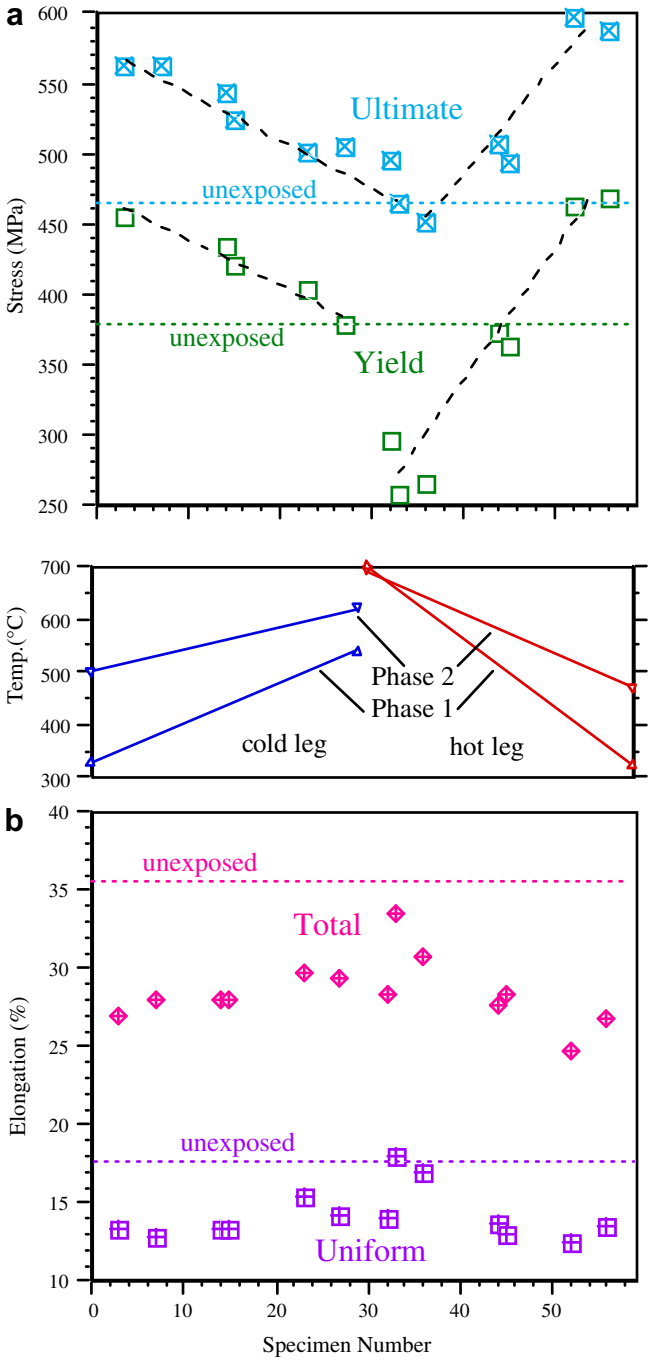

Fig. 3. Room temperature tensile properties of a subset of V–4Cr-4Ti specimens after exposure in a mono-metallic loop: (a) 0.2% yield and ultimate tensile stress and (b) uniform and total elongation. The temperatures assume a linear profile. The specimens in the hottest locations that lost mass showed a decrease in strength and less loss in ductility than the other specimens that had a mass gain after exposure.

Table 2
Measured interstitial composition and mass gain data and calculated mass gain based on the interstitial composition change. The measured mass change is the average of the two tab specimens that were chemically analyzed.

Location	Temperature	Measured change (wppm)			Mass change (mg/cm^2)	
		O	N	C	Measured	Calculated
Top hot leg	657	−340	+1510	+120	−0.50	+0.30
Top cold leg	556	−50	+80	+100	+0.06	+0.03
Middle hot leg	532	−70	+230	+90	+0.06	+0.06
Middle cold leg	487	−30	+30	+70	+0.04	+0.02
Bottom cold leg	423	−40	+30	+20	+0.09	+0.002
Bottom hot leg	416	−40	+30	+10	+0.12	0.0
Starting content		360	80	70		

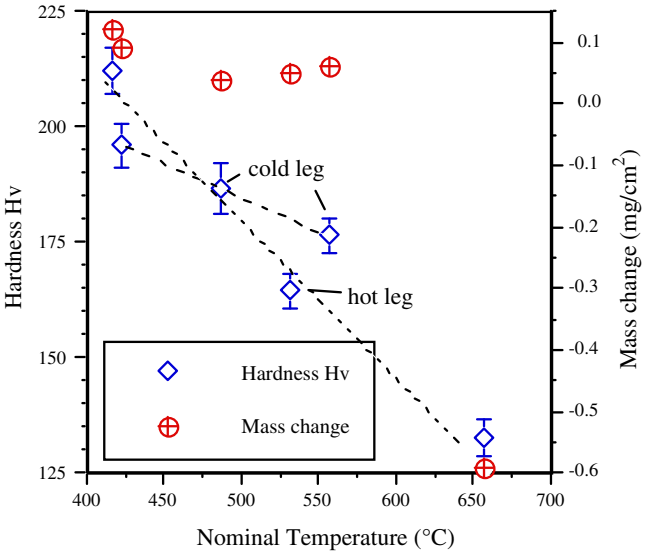

Fig. 4. Average hardness measurements as a function of nominal exposure temperature along the hot and cold legs of the mono-metallic loop. The hardness decreased with exposure temperature in both legs.

assuming a linear temperature change between the thermal wells on the hot and cold legs. The hardness, but not the net mass change, showed a correlation with exposure temperature. Hardness values and standard deviations are based on 7 measurements across the polished ~0.9mm tab cross-section. The decrease in hardness with temperature is consistent with thermal annealing of the original cold-rolled microstructure of the tab specimens. Fig. 5 shows etched metallographic cross-sections of two of the hot leg tab specimens from Fig. 4 and Table 2 with the surface at the top of each figure. The specimen exposed at ~655 °C (Fig. 5(b)) showed a much larger re-crystallized grain size and a surface layer which appeared to be depleted in precipitates. A similar layer or recrystallization was not observed in the other five specimens. The near-surface microhardness has not been investigated yet. Prior work, showed a ~30 μm deep microhardness gradient in V–15Cr–5Ti after exposure at 482–538 °C [19].

Finally, Table 1 shows the profilometry data for the EB-PVD coatings after exposure. Batch 1 coatings were exposed at the higher temperatures because they were of higher initial quality [16]. No

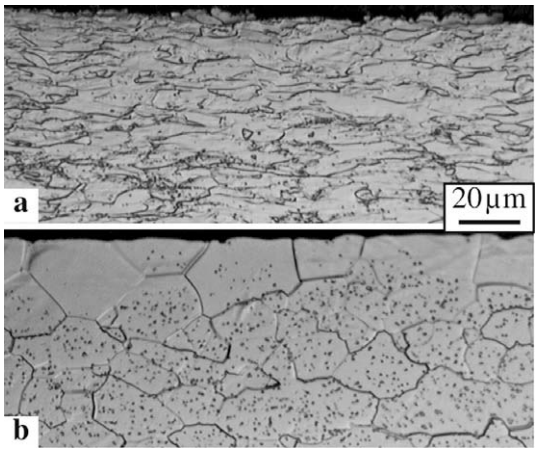

Fig. 5. Light microscopy of V–4Cr–4Ti tab specimens after exposure to flowing Li. (a) Bottom of the hot leg (~415 °C). (b) Top of the hot leg (~655 °C) where the surface grains appear depleted in precipitates. These specimens were not annealed prior to exposure.

significant loss in thickness was detected. However, the unexposed coated specimens were concave indicating that the as-deposited coatings were under compression while the coated specimens exposed at the highest temperatures were all convex after exposure which could indicate stress relief or some type of degradation such as cracking or expansion due to reaction with Li. A procedure is being developed to electrically isolate the oxide coating in order to measure the post-exposure electrical resistance.

4. Summary

A mono-metallic V–4Cr–4Ti thermal convection loop was run for 2355 h with a maximum temperature of 700 ± 10 °C to determine the compatibility of V–4Cr–4Ti and Y_2O_3/V coatings with flowing (~2–3 cm/s) Li. Small mass losses (equivalent to ⩽1.3 μm of metal loss) were measured at the top of the hot leg. Elsewhere, small mass gains were measured. Specimens that gained mass also showed an increase in yield stress and modest decrease in ductility consistent with the observed increase in N and C contents. The EB-PVD Y_2O_3/V coatings showed no significant loss in thickness, however, further characterization is needed to determine their electrical resistance and microstructure after exposure.

Acknowledgments

This research was sponsored by the Office of Fusion Energy Sciences, US Department of Energy (DOE), under contract DE-AC05-00OR22725 with UT-Battelle, LLC and the JUPITER-II Japan-US collaboration on fusion blanket systems and materials. T. Brummett, R. Parten and H. Longmire assisted with the experimental work. D.F. Wilson, M. Li, S.J. Zinkle and R. Stoller provided comments on the manuscript.

References

[1] R.J. Kurtz, K. Abe, V.M. Chernov, D.T. Hoelzer, H. Matsui, T. Muroga, G.R. Odette, J. Nucl. Mater. 329–333 (2004) 47.
[2] T. Muroga, J.M. Chen, V.M. Chernov, K. Fukumoto, D.T. Hoelzer, R.J. Kurtz, T. Nagasaka, B.A. Pint, M. Satou, A. Suzuki, H. Watanabe, J. Nucl. Mater. 367–370 (2007) 780.
[3] I.R. Kirillov, C.B. Reed, L. Barleon, K. Miyazaki, Fus. Eng. Des. 27 (1995) 553.
[4] L. Barleon, V. Casal, L. Lenhart, Fus. Eng. Des. 14 (1991) 401.
[5] S. Malang, H.U. Borgstedt, E.H. Farnum, K. Natesan, I.V. Vitkovski, Fus. Eng. Des. 27 (1995) 570.
[6] L. Bühler, Fus. Eng. Des. 27 (1995) 650.
[7] Y.Y. Liu, D.L. Smith, J. Nucl. Mater. 141–143 (1986) 38.
[8] J.E. Battles, Int. Mater. Rev. 34 (1989) 1.
[9] T. Terai et al., J. Nucl. Mater. 233–237 (1996) 1421.
[10] B.A. Pint, P.F. Tortorelli, A. Jankowski, J. Hayes, T. Muroga, A. Suzuki, O.I. Yeliseyeva, V.M. Chernov, J. Nucl. Mater. 329–333 (2004) 119.
[11] B.A.PintJ.L. Moser, P.F. Tortorelli, Fus. Eng. Des. 81 (2006) 901.
[12] B.A. Pint, J.L. Moser, A. Jankowski, J. Hayes, J. Nucl. Mater. 367–370 (2007) 1165.
[13] I.V. Vitkovsky et al., Fus. Eng. Design 61&62 (2002) 739.
[14] D.L. Smith, H.M. Chung, B.A. Loomis, H.-C. Tsai, J. Nucl. Mater. 233–237 (1996) 356.
[15] M.L. Grossbeck, J.F. King, T. Nagasaka, S.A. David, J. Nucl. Mater. 307–311 (2002) 1590.
[16] A.F. Jankowski, B.A. Pint, unpublished research (2007).
[17] B.A. Pint, et al., DOE-ER-0313/41 (2006) 2.
[18] B.A. Pint, et al., DOE-ER-0313/42 (2007) 2.
[19] O .K. Chopra, D.L. Smith, J. Nucl. Mater. 155–157 (1988) 683.
[20] V.A. Evtikhin, I.E. Lyublinski, A.V. Vertkov, J. Nucl. Mater. 258–263 (1998) 1487.
[21] H.M. Chung, B.A. Loomis, D.L. Smith, Fus. Eng. Des. 29 (1995) 455.
[22] K. Fukumoto, T. Morimura, T. Tanaka, A. Kimura, K. Abe, H. Takahashi, H. Matsui, J. Nucl. Mater. 239 (1996) 170.
[23] B.A. Pint, J.R. DiStefano, Oxid. Met. 63 (2005) 33.
[24] T. Nagasaka, T. Muroga, M.M. Li, D.T. Hoelzer, S.J. Zinkle, M.L. Grossbeck, H. Matsui, Fus. Eng. Des. 81 (2006) 307.